



University of Batna 2, Algeria
Faculty of Technology
Department of mechanical engineering



5th INTERNATIONAL CONFERENCE

ON ADVANCES IN MECHANICAL ENGINEERING ISTANBUL 2019

ICAME2019



JOURNAL OF THERMAL ENGINEERING



17 – 19 December

**Numerical Study of Air-Air Mixing in Turbulent Compressible
Coaxial Jets: effect of hot jet**

Mohamed SI-AMEUR

Outline

- **The Context and applications**
- **The mathematical model and numerical procedure**
- **Monotone Integrated Large Eddy Simulations(MILES)**
- **Results and discussion**



Applications:

- commercial applications such as abrasive blasting
 - gas pipelines
 - high speed aircraft and jet engines

The Numerical method is based on High order Godunov's scheme called PPM (piecewise parabolic method) combined with lineared Riemann solver.

$$\frac{\partial U(\vec{X}, t)}{\partial t} + \sum_{j=1}^2 \frac{\partial F_j(U(\vec{X}, t))}{\partial X_j} = S(U(\vec{X}, t))$$

• Equations for conservation of mass, momentum, energy an detailed mass of each species i are written in conservative form

• The overall scheme is 2nd order accurate in time

• A diffusion reaction operator is added as a source term in Navier-Stokes equations

$$U(\vec{X}, t) = \{\rho, \rho U_1, \rho U_2, \rho U_3, \rho e, \rho Y_i\}^T$$

-The developed code : simulate gas flows whose composition may evolve with location and time

-The code is based on the usual set of gas flow equations with the vector of the conserved variable

$$F_j(U(\vec{X}, t)) = \left\{ \begin{array}{c} \rho U_j \\ \rho U_j U_1 + \delta_{j1} P \\ \rho U_j U_2 + \delta_{j2} P \\ \rho U_j U_3 + \delta_{j3} P \\ (\rho e + p) U_j \\ \rho Y_i U_j \\ \dots \end{array} \right\}$$

-Mass flux
 -- Momentum flux
 -- energy flux
 -- species flux

$$S(U) = \left\{ \begin{array}{c} 0 \\ \sum_{j=1}^{j=3} \frac{\partial(\frac{\rho}{Re})\tau_{1j}}{\partial X_j} \\ \sum_{j=1}^{j=3} \frac{\partial(\frac{\rho}{Re})\tau_{2j}}{\partial X_j} \\ \sum_{j=1}^{j=3} \frac{\partial(\frac{\rho}{Re})\tau_{3j}}{\partial X_j} \\ \nabla \cdot \left(\frac{\overline{Cp\rho}}{Pr.Re} \nabla T \right) + \nabla \cdot \left(\frac{\rho}{Re} \vec{U} \cdot \vec{\tau} \right) \\ \nabla \cdot \left(\frac{\rho}{Sc.Re} \nabla Y_i \right) \\ \dots \end{array} \right\}$$

-viscous stress
 -temperature diffusivity
 - scalar diffusivity

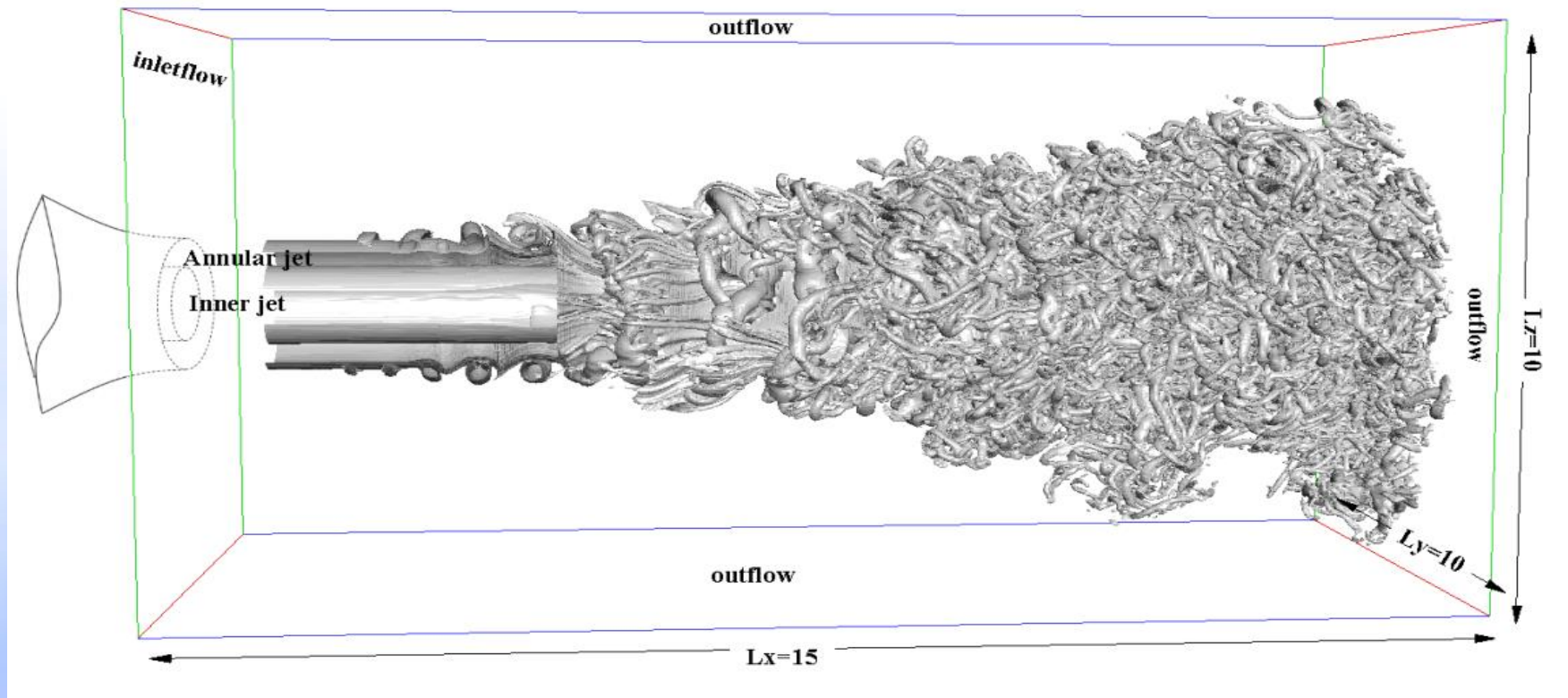
The full compressible Navier-Stokes equations (4) are split up in three one-dimensional inviscid operators L_j ($j=1,3$):

and three-dimensional viscous-diffusive operator :

$$L_j : \frac{\partial U(\vec{X}, t)}{\partial t} + \frac{\partial F_j(U(\vec{X}, t))}{\partial X_j} = 0$$

$$\psi : \frac{\partial U(\vec{X}, t)}{\partial t} = S(U(\vec{X}, t))$$

The spatial discretization of equation is done by finite volume. All simulations have been carried out on the same computational grid consisting in 400.400.400 points with a uniform mesh size in all three directions for a domain size of 15D.10D.10D, along the streamwise (x) and the two transverse directions (y, z)

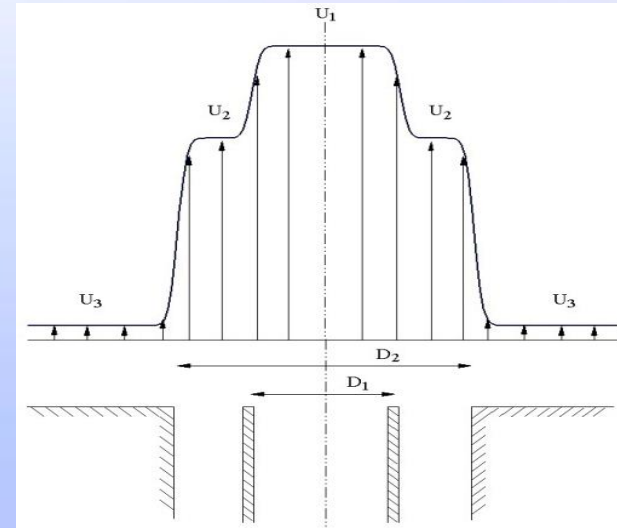
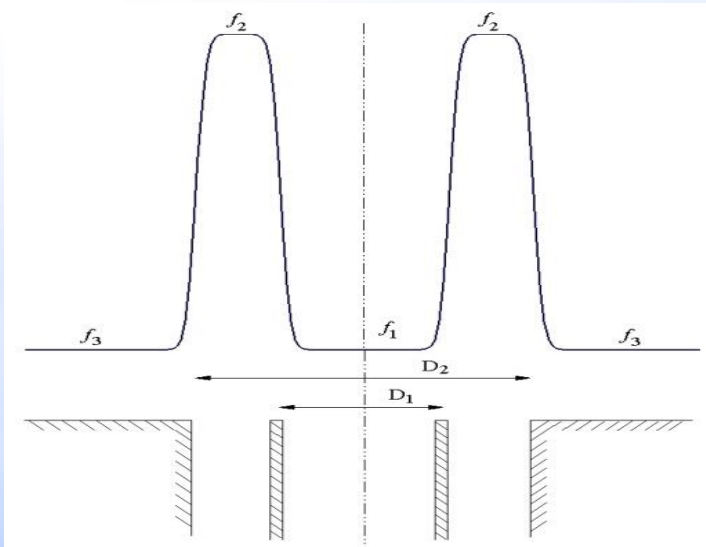


$$\vec{U}(\vec{x}_0, t) = \vec{U}_{med}(\vec{x}_0) + \vec{U}_{noise}(\vec{x}_0, t)$$

-The shape of the inlet velocity profil: based on two hyperbolic tangent profil as the main instabilities are conditionned by the mean velocity profile at the nozle.

-A random noise superimposed on the inlet profile to model the residuel turbulence near the the nozle exit

-- A temperature profile based on Croco-Buseman's equation is imposed



$$f(x=0, r, \phi) = \begin{cases} \frac{f_1 + f_2}{2} + \frac{f_1 - f_2}{2} \tanh\left(\frac{r - R_1}{2\theta_{01}}\right) & \text{for } r \leq R_m \\ \frac{f_1}{2} + \frac{f_2}{2} \tanh\left(\frac{r - R_2}{2\theta_{02}}\right) & \text{for } r > R_m \end{cases}$$

$$U_{med}(\vec{x}_0 = (0, r, \phi)) = \begin{cases} \frac{U_1 + U_2}{2} + \frac{U_1 - U_2}{2} \tanh\left(\frac{r - R_1}{2\theta_{01}}\right) & \text{for } r \leq R_m \\ \frac{U_2 + U_3}{2} + \frac{U_2 - U_3}{2} \tanh\left(\frac{r - R_2}{2\theta_{02}}\right) & \text{for } r > R_m \end{cases}$$

Sketch of the inlet profile. a) The velocity profile U1 is the inner jet velocity coming out of the nozzle

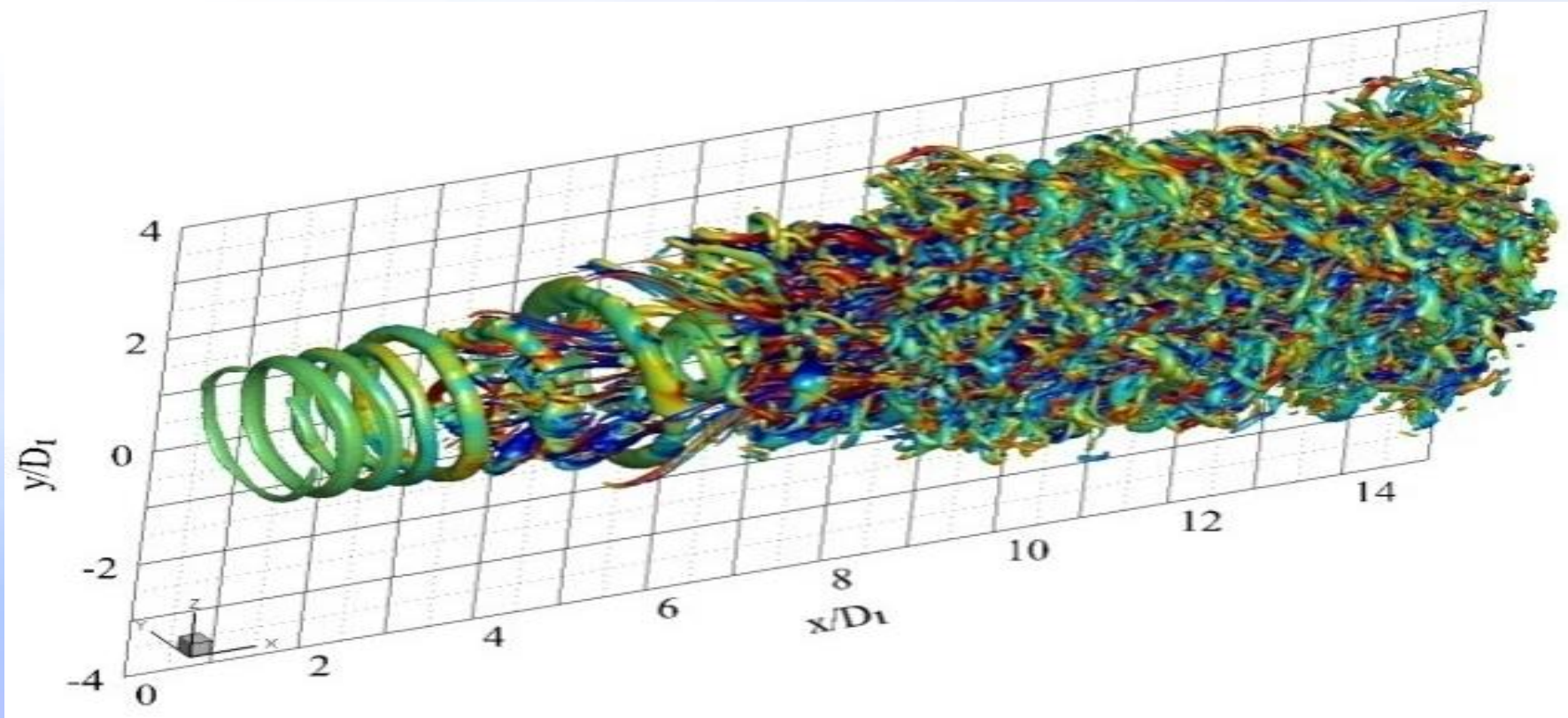
(diameter D1), U2 is the velocity

of the outer jet stream, issuing from a diameter D2 = 2 D1. b) The inlet mixture fraction we seed species (f1 = 1)

either into outer the jet and (f2 = 0) into inner

		Parameters	Cold Coaxial Jet	Hot coaxial jet
Inner jet	velocity (m/s)		175	282
	Temperature (°K)		293.15	792
	Mach number		0.5	0.5
	Reynolds number		6.25×10^5	6.25×10^5
Annular jet	velocity (m/s)		120.5	197.4
	Temperature (°K)		293.15	293.15
	Mach number		0.35	0.57

Table : summarizes the flow parameters.

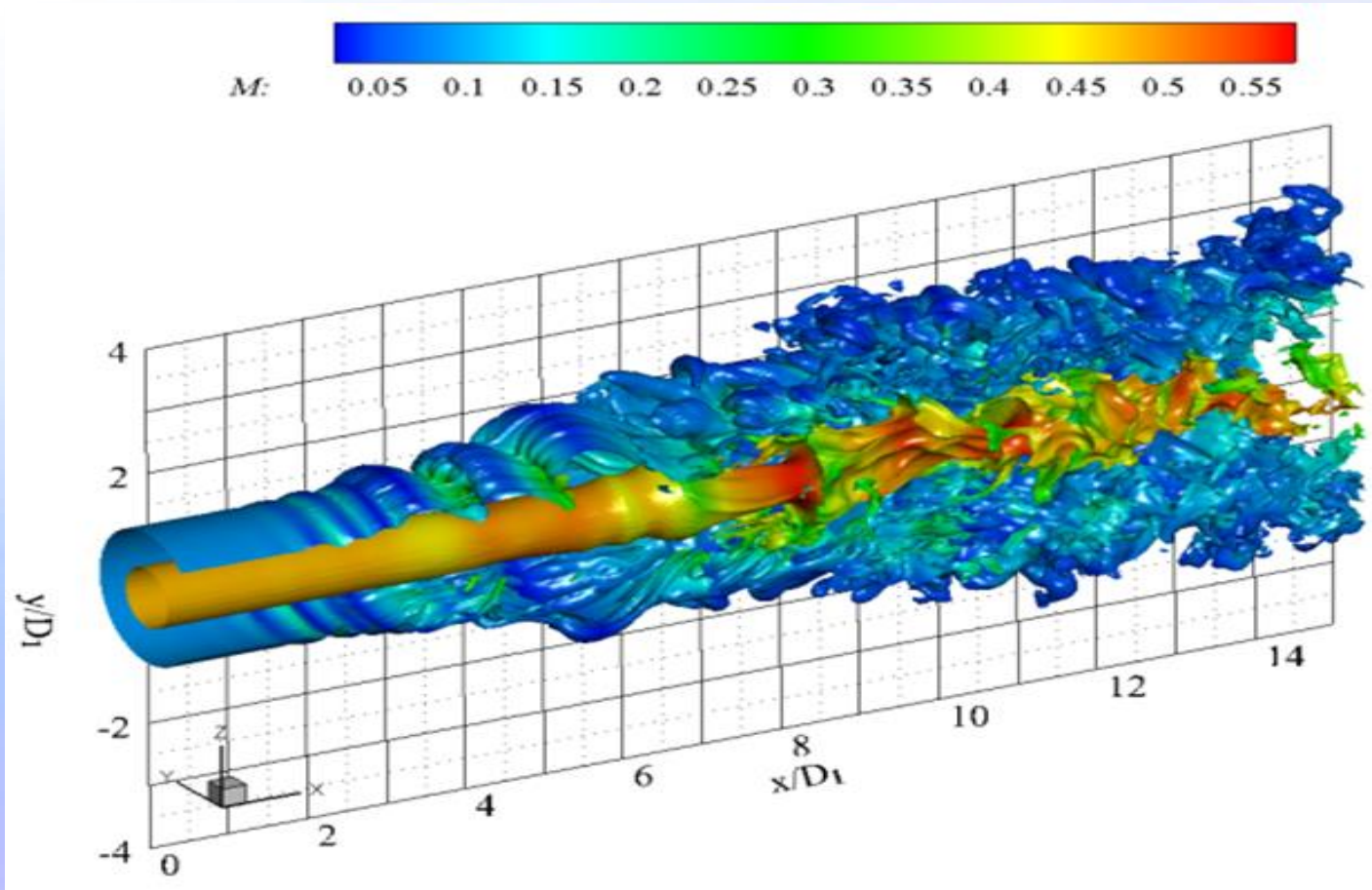


Global view of natural isothermal coaxial jet case; Positive Q isosurfaces colored by the streamwise vorticity ω_x .

Q is second invariant of the velocity-gradient tensor.

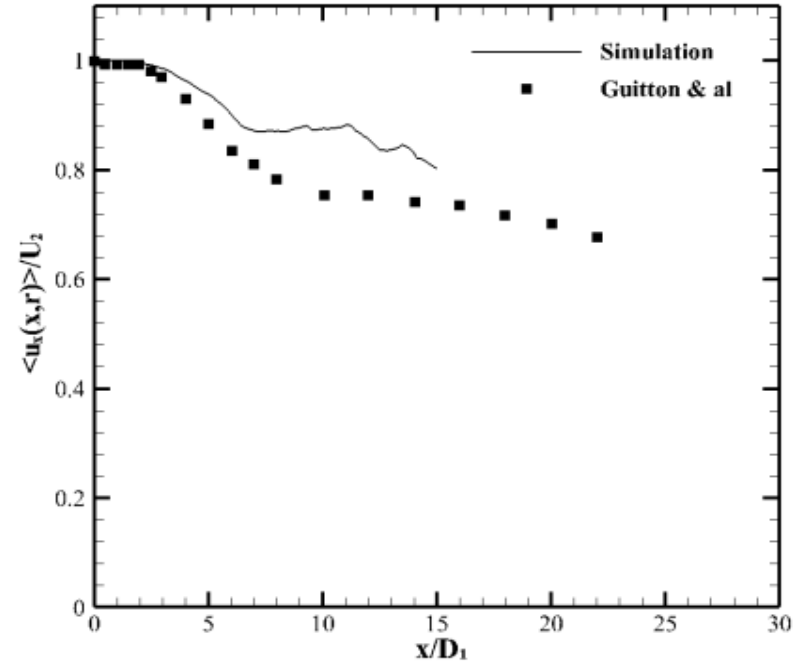
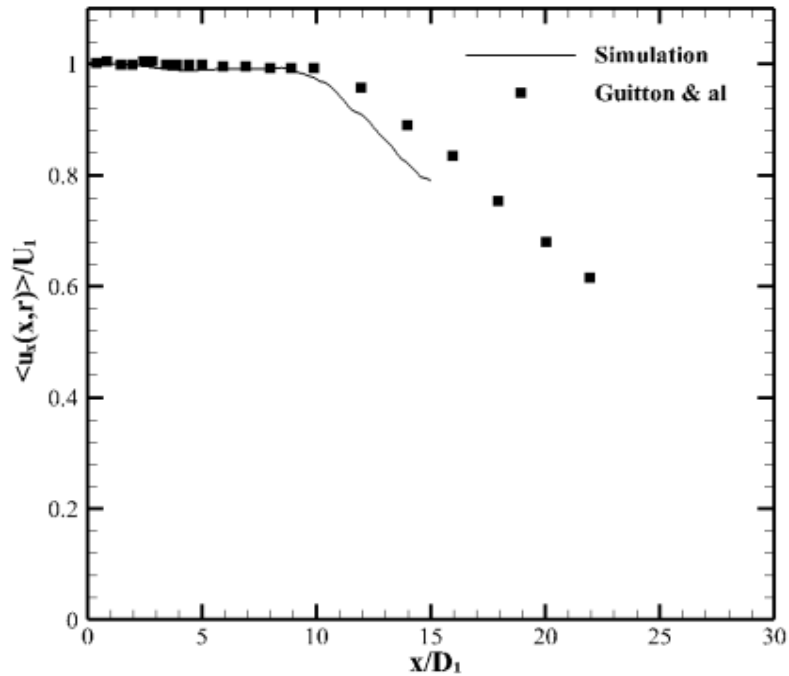
The outer shear layers roll up into-quasi axisymmetric vortex rings due to Kelvin-Helmoltz instabilities.

Delay in the development of the inner shear layer



Global view of natural isothermal coaxial jet case; $f = 0.15$ mixture-fraction isosurface colored by the Mach field.

The first streamwise vortices begin to form between two primary structures. They appear by counter-rotating pairs in agreement with the classical scenario of transition in free shear layers. The vortex stretching phenomena leading to streamwise vortices begins earlier for the outer shear layer



Downstream evolution of the axial mean velocity: a) In the inner ($r/D_1=0$). b) In the outer ($r/D_1=0.75$) jets. The numerical results are compared with the measurements by Guitton & al.

In order to compute the turbulence intensities, the relation:

$$\varphi' = \sqrt{\overline{\varphi^2} - 2\overline{\varphi} \frac{\overline{\rho\varphi}}{\rho} + \frac{\overline{\rho\varphi}^2}{\rho}}$$

is used. The temporal average: .

$$\overline{\varphi}(x, y, z) = \frac{1}{T} \int_{t_0}^{t_0+T} \varphi(x, y, z, t) dt$$

Where : $\varphi(x, y, z) = U_{i=1,2,3}$

The potential cones of the primary and secondary jets are clearly distinguished. It is observed that the potential cone of the primary jet is considerably longer than that of the secondary jet

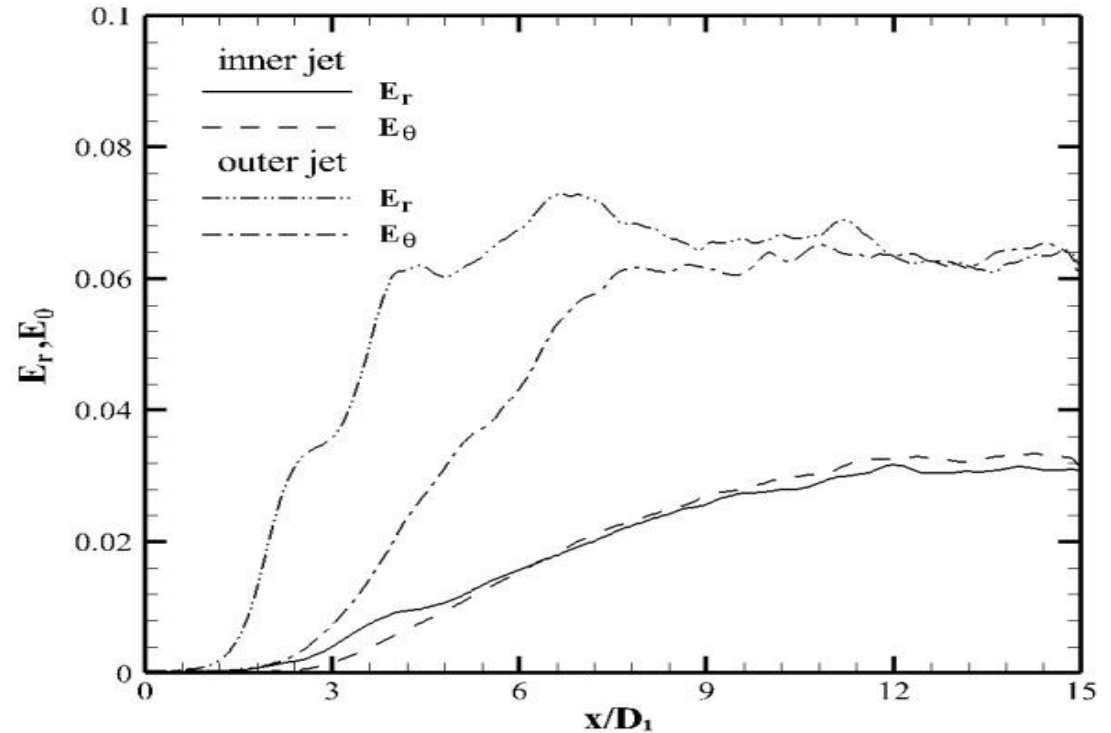
$$E_r(x) = \sqrt{\frac{2\pi}{L_y L_z} \int_0^{R_m} \langle u_r'^2 \rangle(x, r) r dr}$$

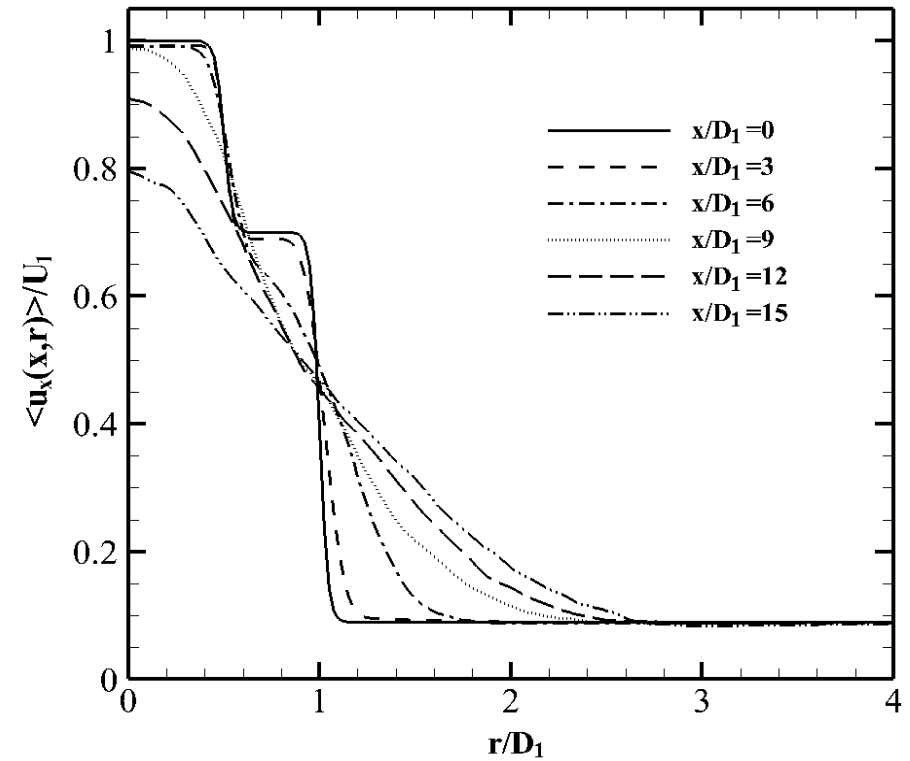
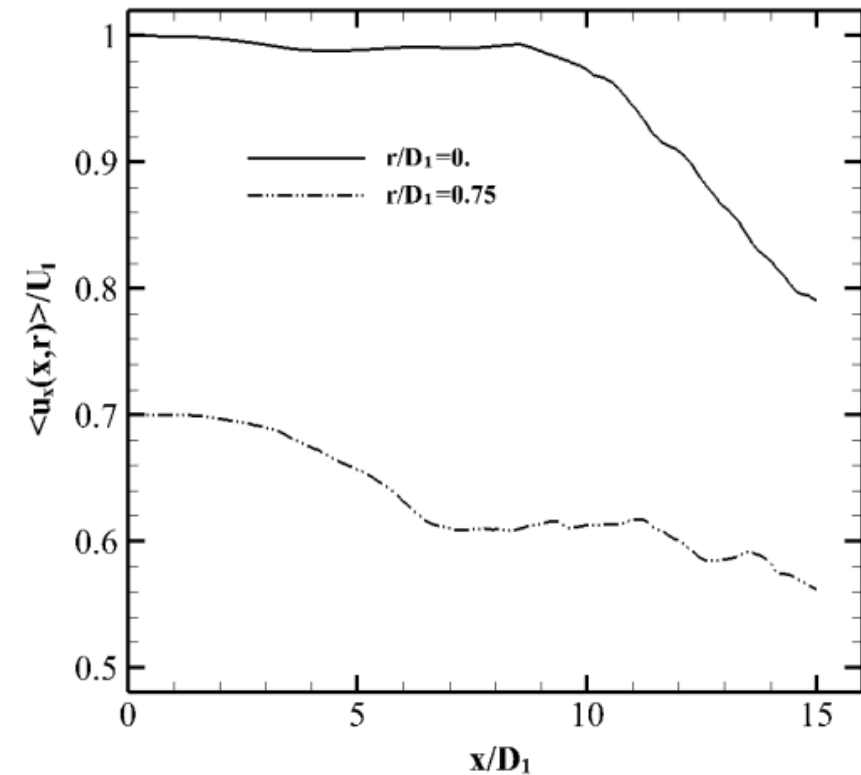
$$E_\phi(x) = \sqrt{\frac{2\pi}{L_y L_z} \int_0^{R_m} \langle u_\phi'^2 \rangle(x, r) r dr}$$

For the inner shear layer

$$E_r(x) = \sqrt{\frac{2\pi}{L_y L_z} \int_0^{R_m} \langle u_r'^2 \rangle(x, r) r dr}$$

$$E_\phi(x) = \sqrt{\frac{2\pi}{L_y L_z} \int_{R_m}^{\infty} \langle u_\phi'^2 \rangle(x, r) r dr}$$

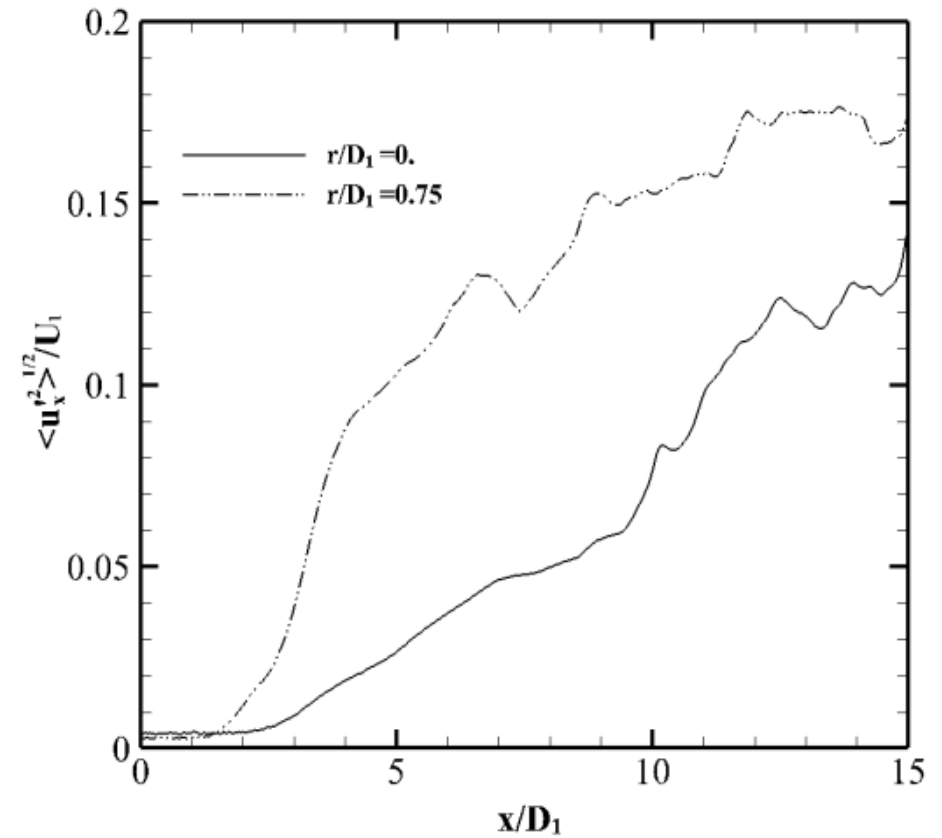
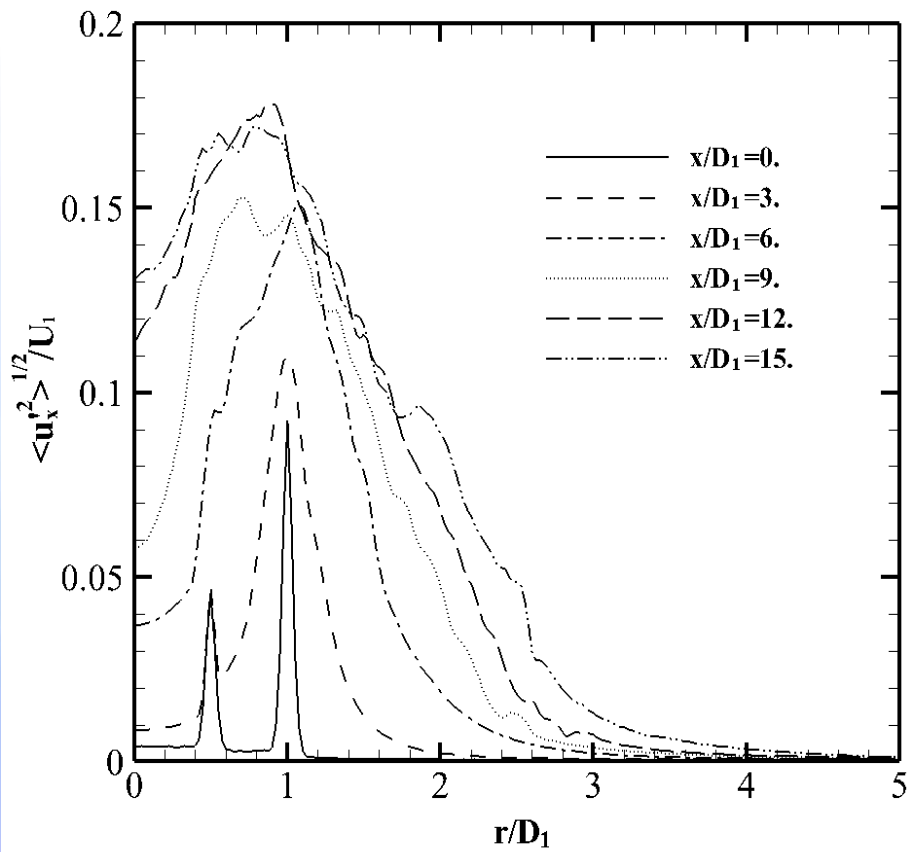




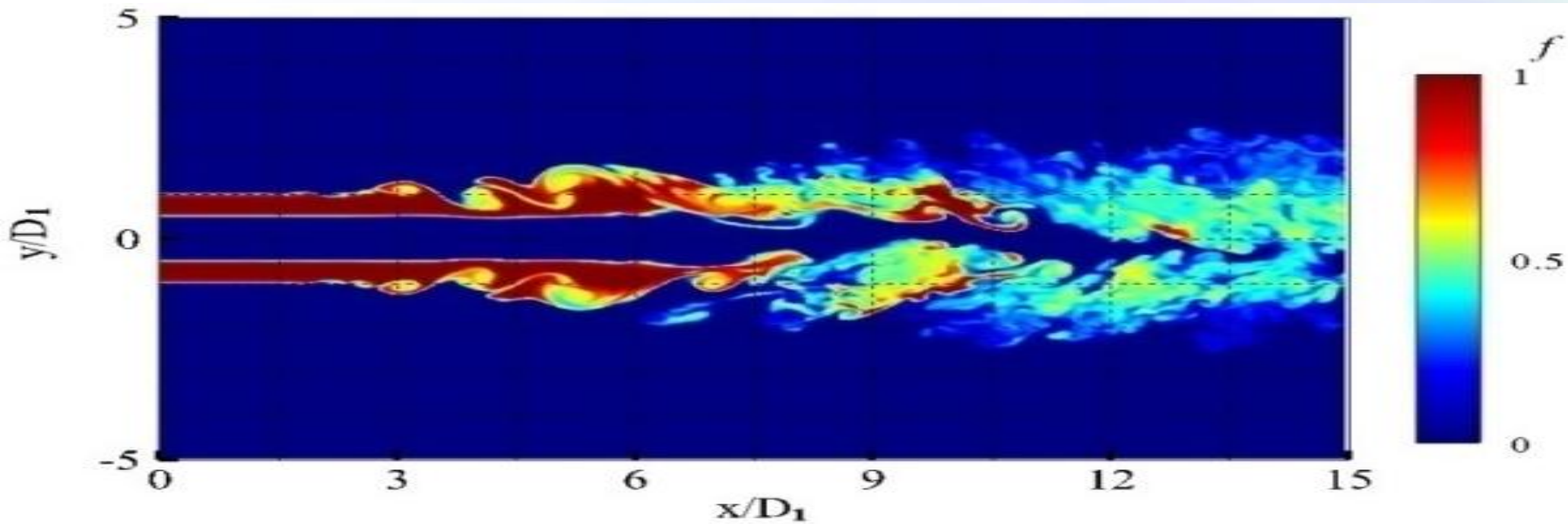
• **Mean axial velocity component. a) Downstream evolution**

in both central and annular jets. The evolution of the axial velocity after the end of each potential core is governed by radial diffusion of linear momentum which transfers momentum from the outer into the inner shear layers.

- **This idea is confirmed in figure) showing profiles of axial velocity at several stations for this case. Notice that for $x/D_1 = 9$ the velocity profile has lost its two-layer structure, and the maximum velocity is located at the centreline.**

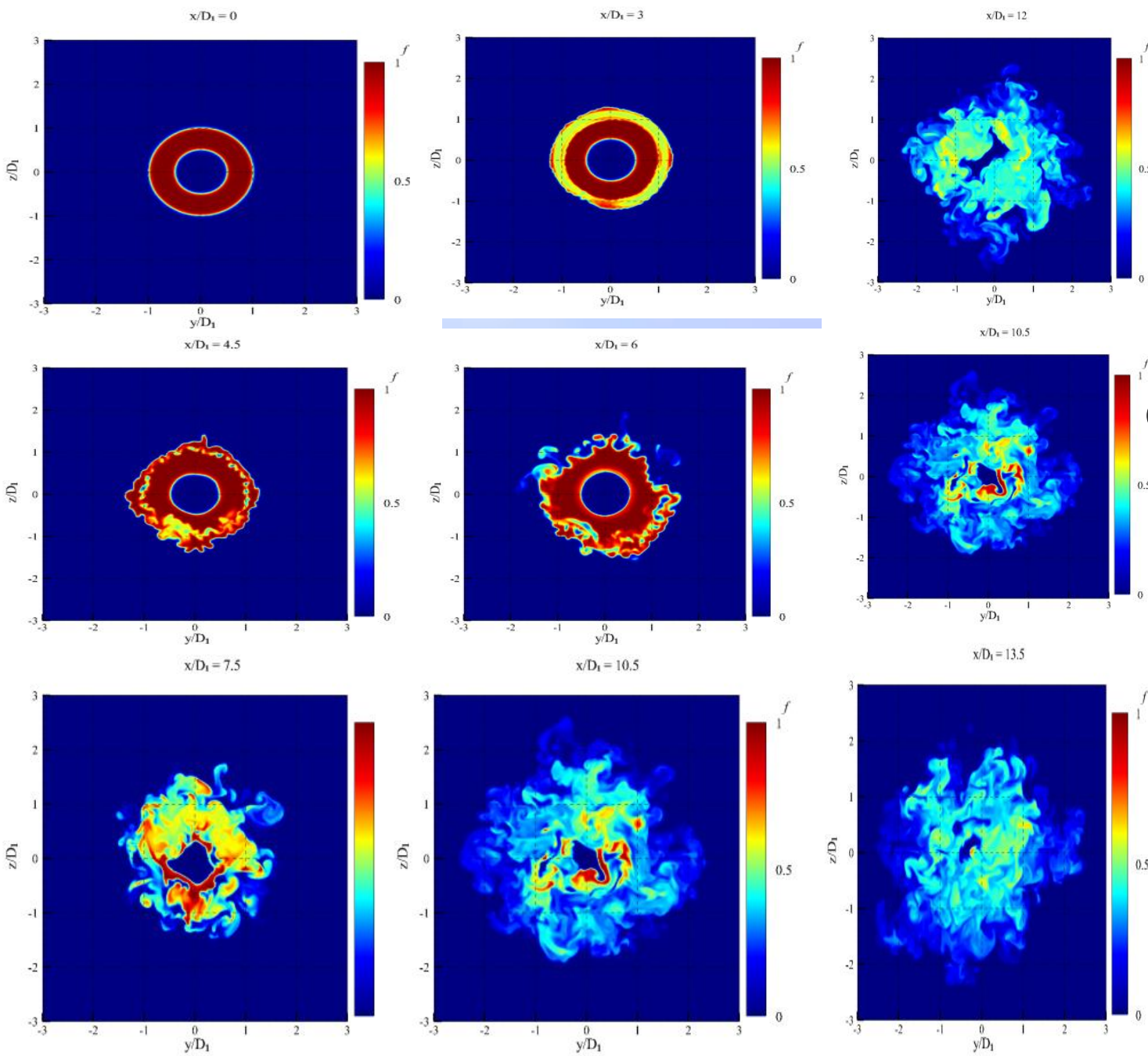


Rms of the longitudinal velocity fluctuation. a) Radial evolution at several downstream locations. b) Downstream evolution in both central and annular jets.

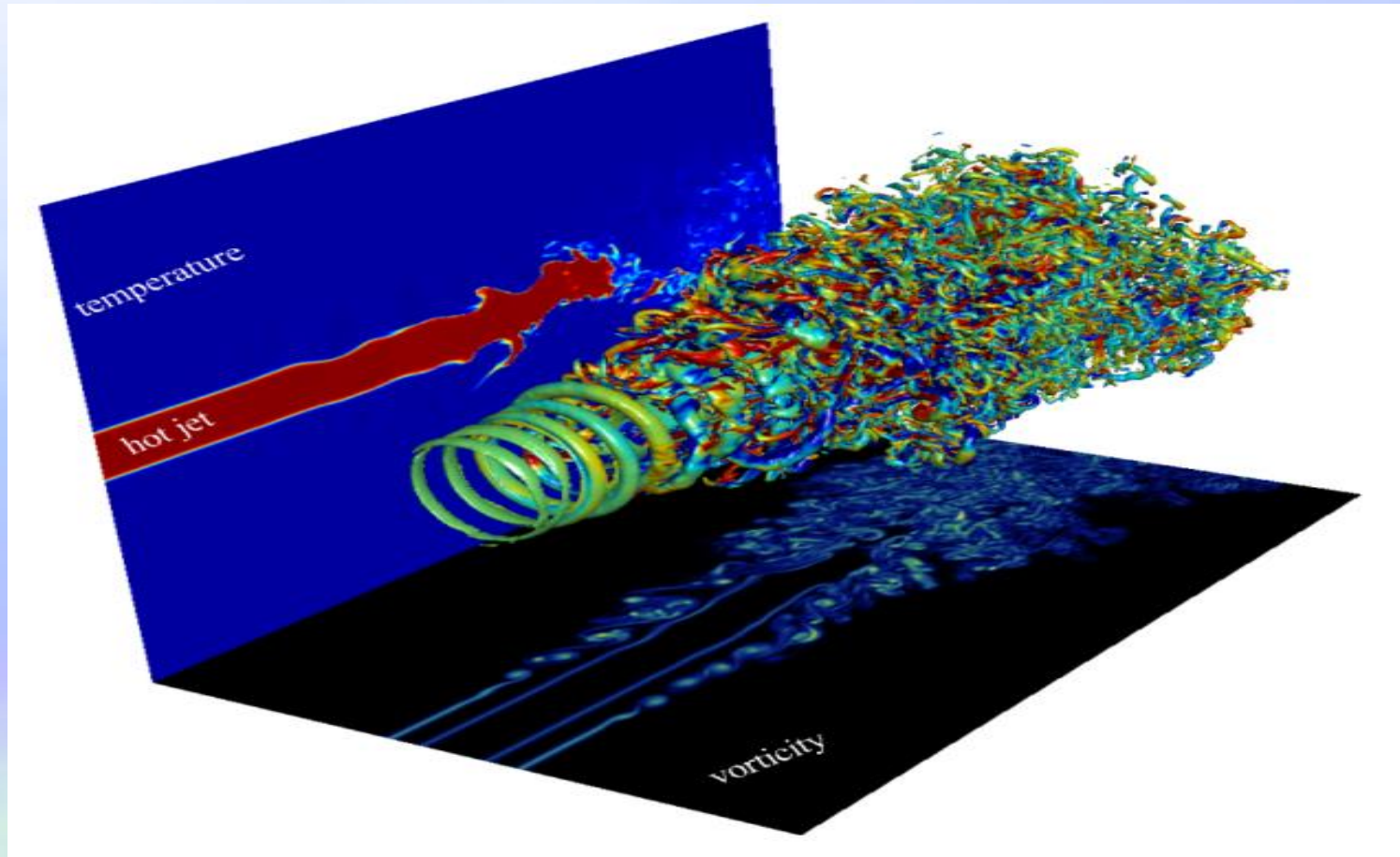


□ Contours for the natural isothermal jet in the central plane: mixture fraction.

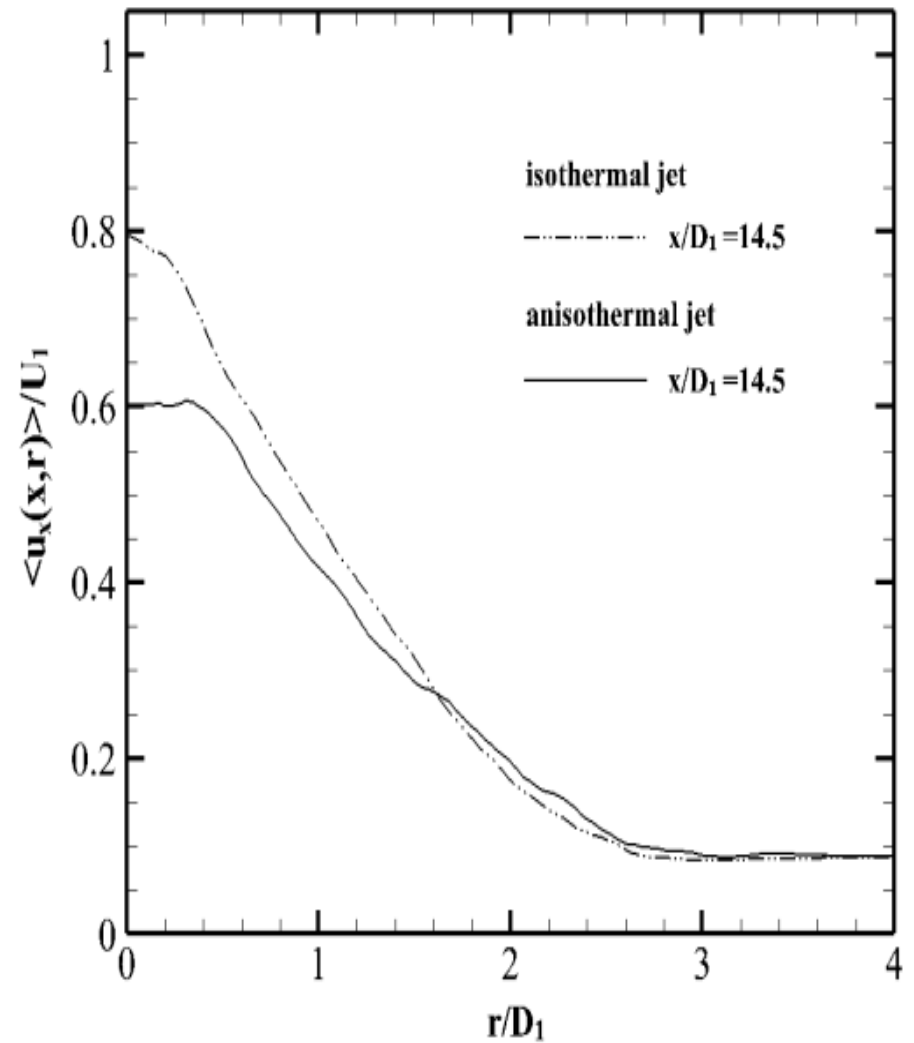
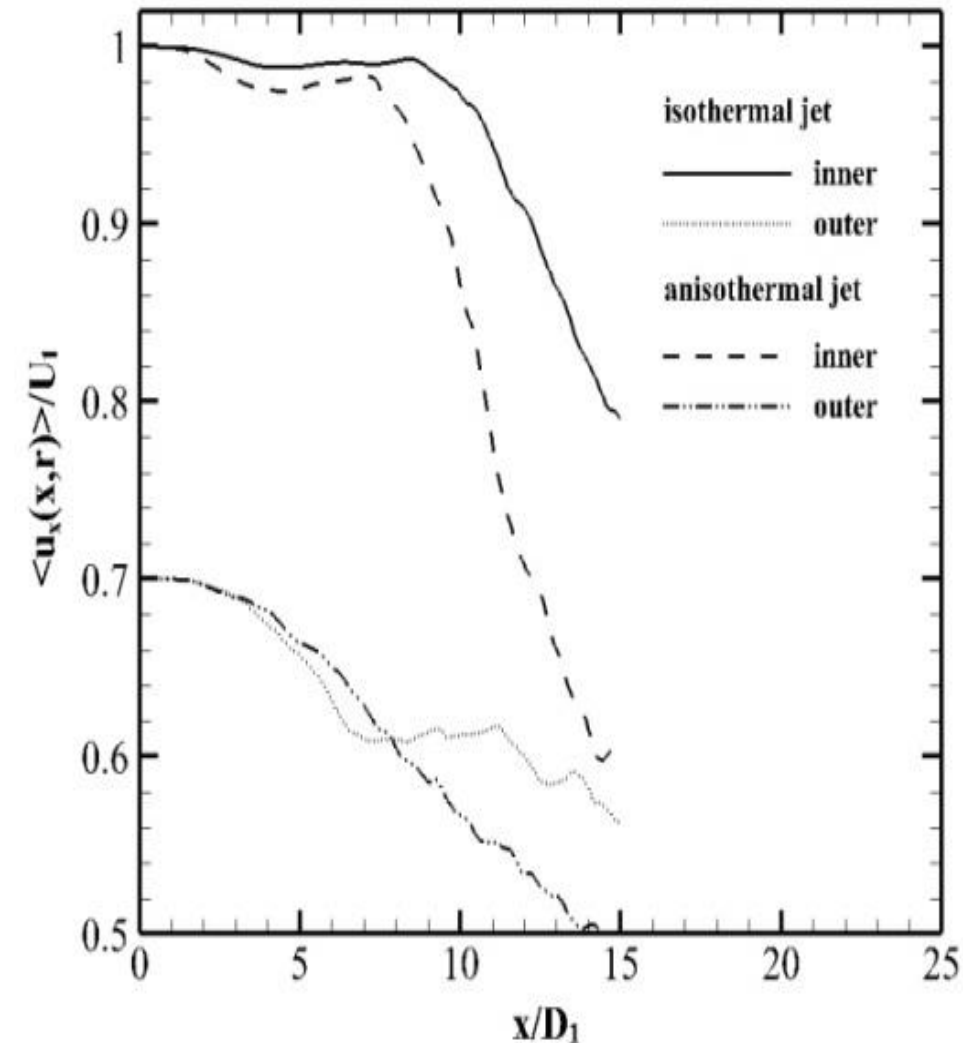
□ Characterization of the multi-scale geometry of the iso-species surfaces is a crucial step for understanding and modeling turbulent mixing linked to turbulent combustion processes. The mixture-fraction isosurface is highly convoluted after the instabilities amplification, with evidence of a large-scale structure. Thus, the inner and outer Kelvin–Helmholtz vortices allow for an engulfment of the two fluid streams placed on each side of the inner and outer shear



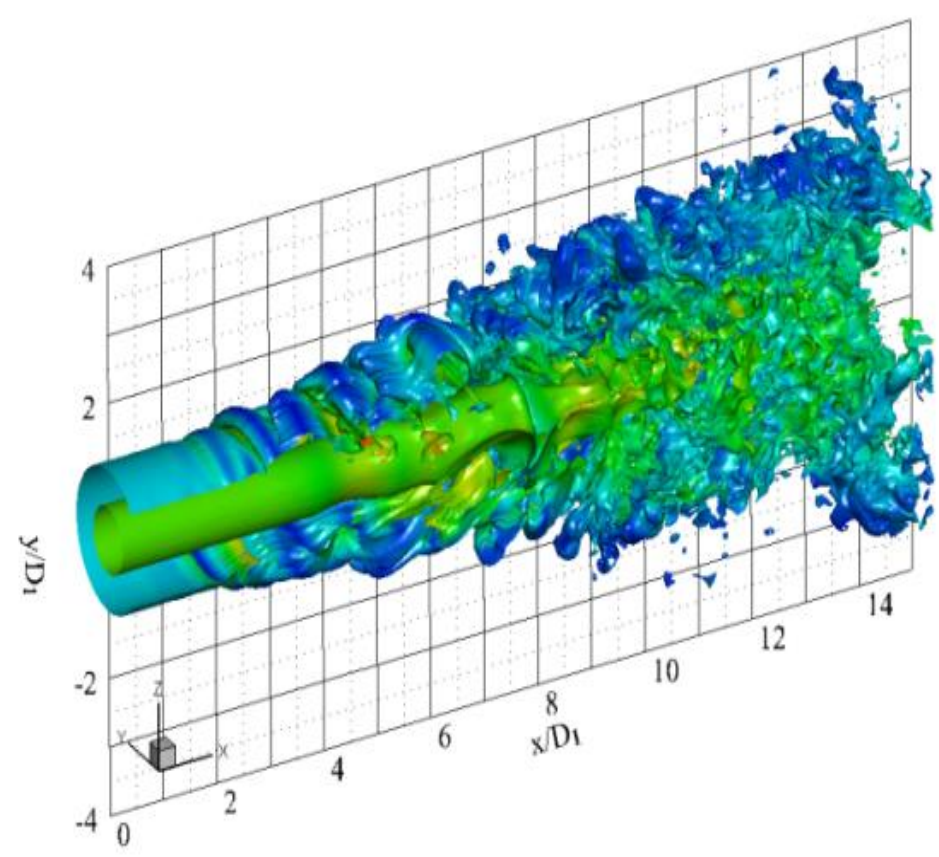
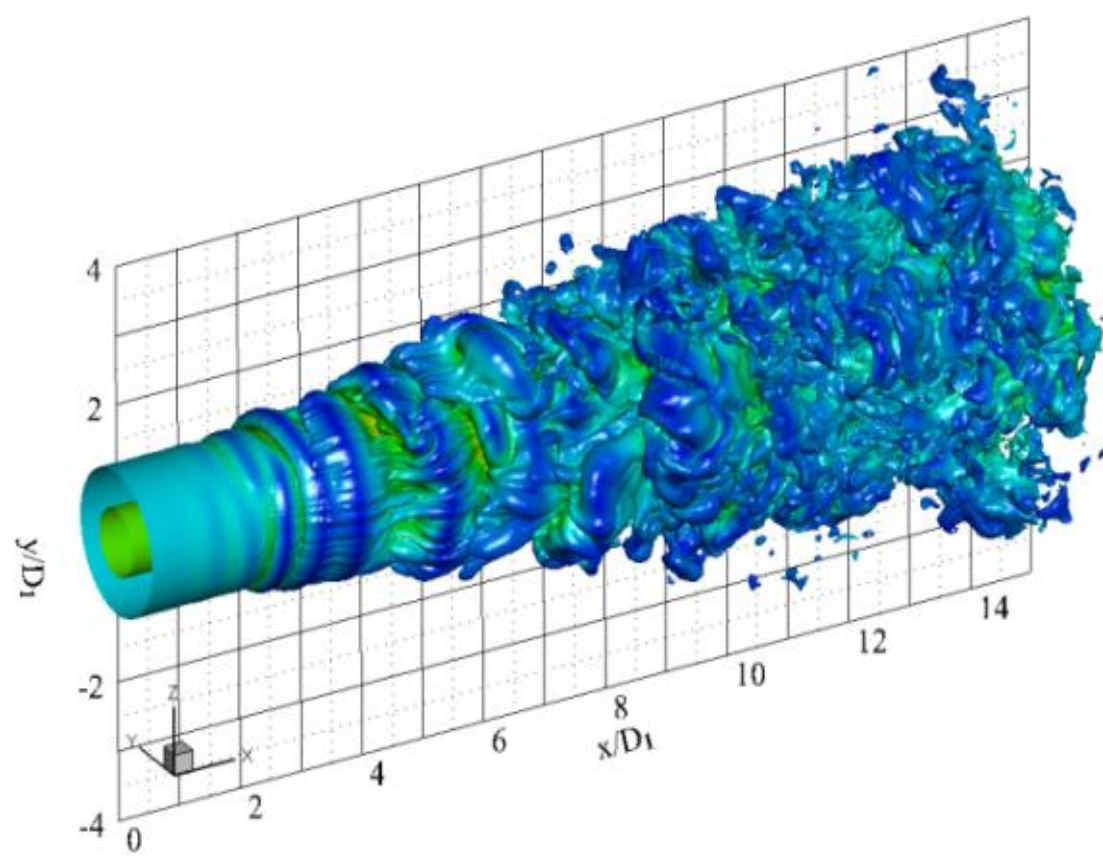
**Cut through the (z, y)
plane of the mixture
fraction fields.**



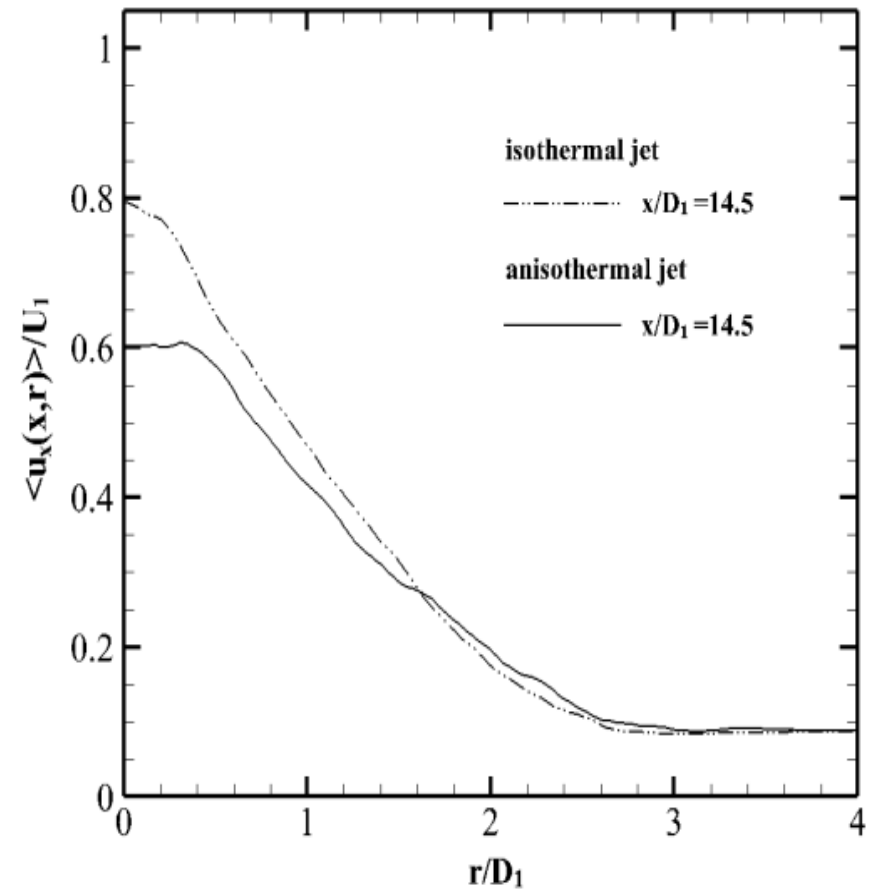
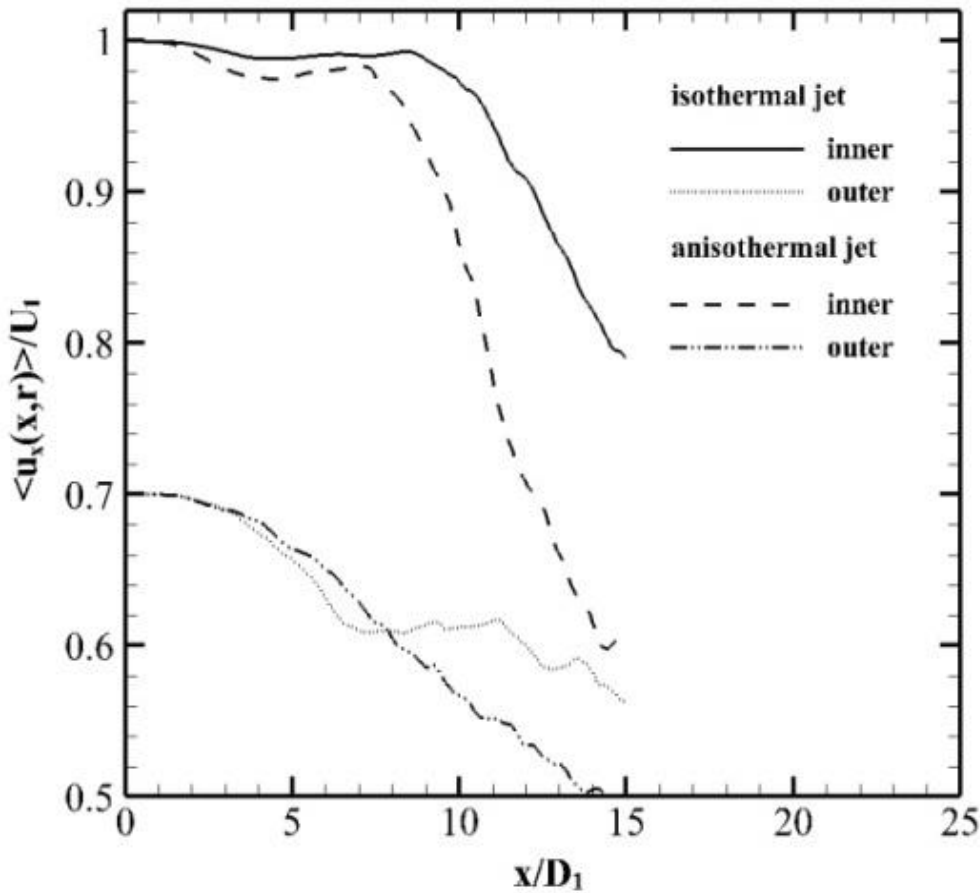
Positive Q isosurfaces colored by the streamwise vorticity ω_x , for anisothermal



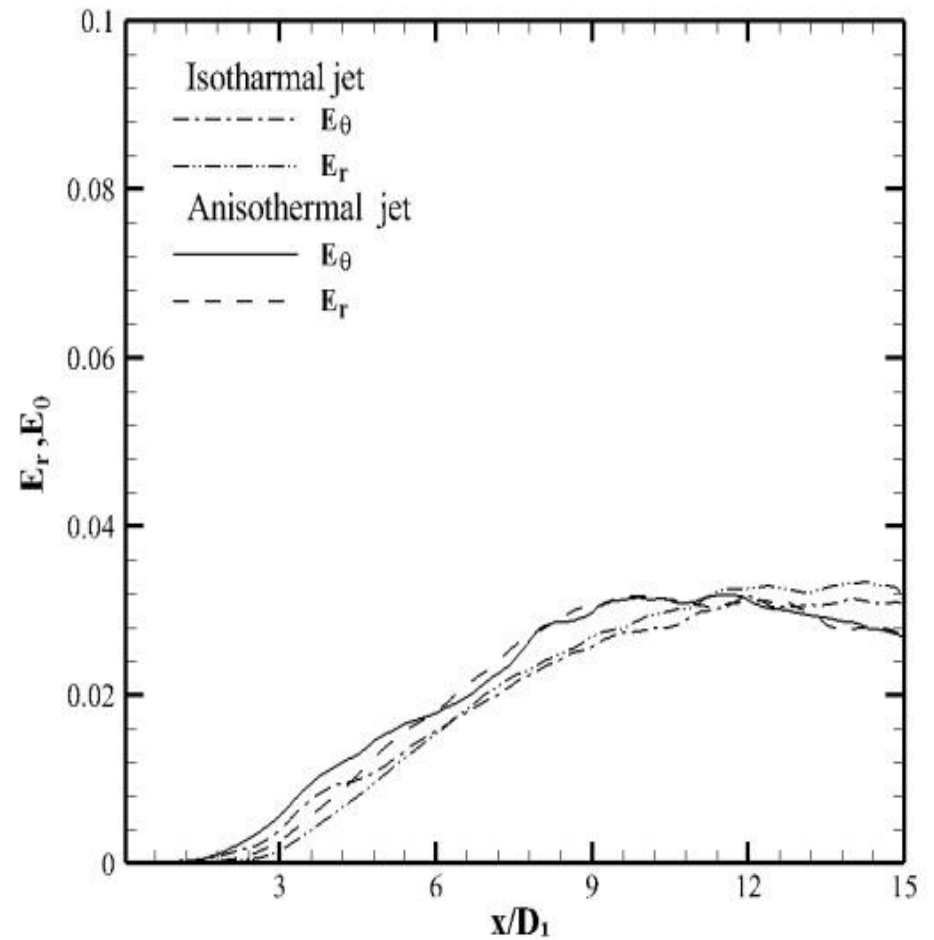
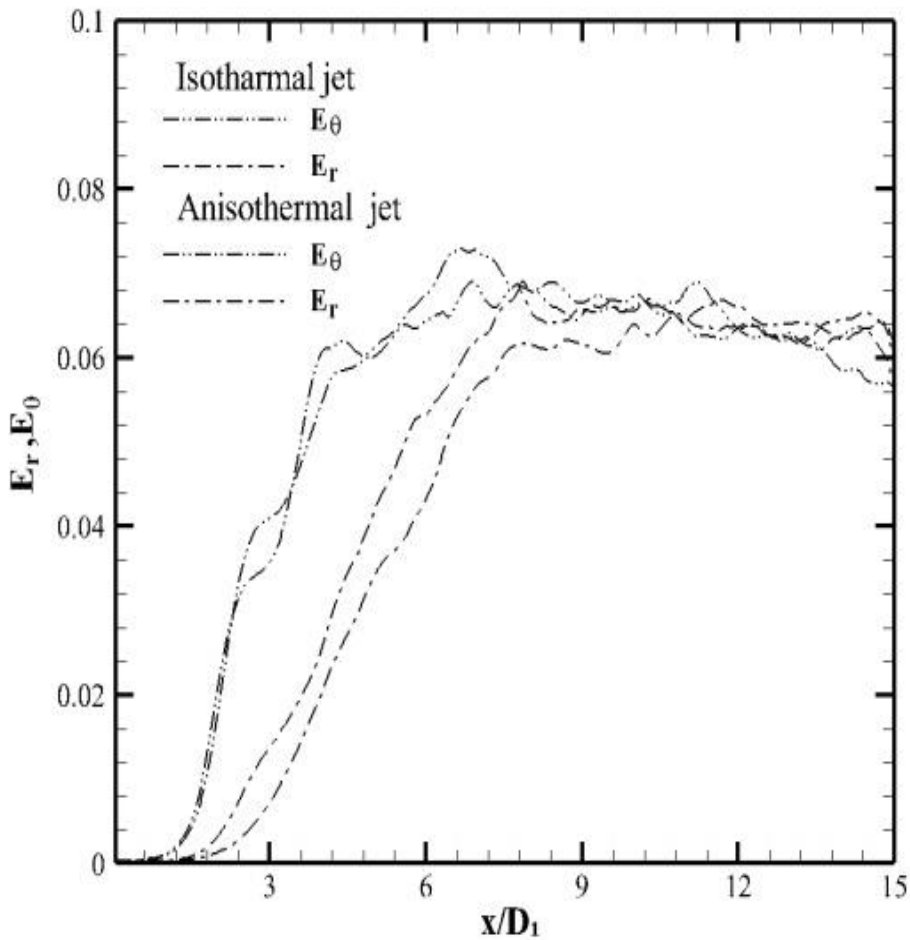
Comparison of the mean velocity between isothermal and anisothermal jet cases: (a) downstream evolution in the inner ($r/D_1=0$) and outer ($r/D_1=0.75$) jets and (b) profiles at several downstream locations ($x/D_1=14.5$).



Isosurface of mixture-fraction colored by the Mach field. b) Cut view of mixture-fraction isosurface colored by the Mach field, for anisothermal case.



Comparison of the mean velocity between isothermal and anisothermal jet cases:
(a) downstream evolution in the inner ($r/D_1=0$) and outer ($r/D_1=0.75$) jets and (b) profiles at several downstream locations ($x/D_1=14.5$).



Downstream evolution of the radial and azimuthal contributions to turbulent kinetic energy calculated in the outer (a) and inner (b) shear layers.

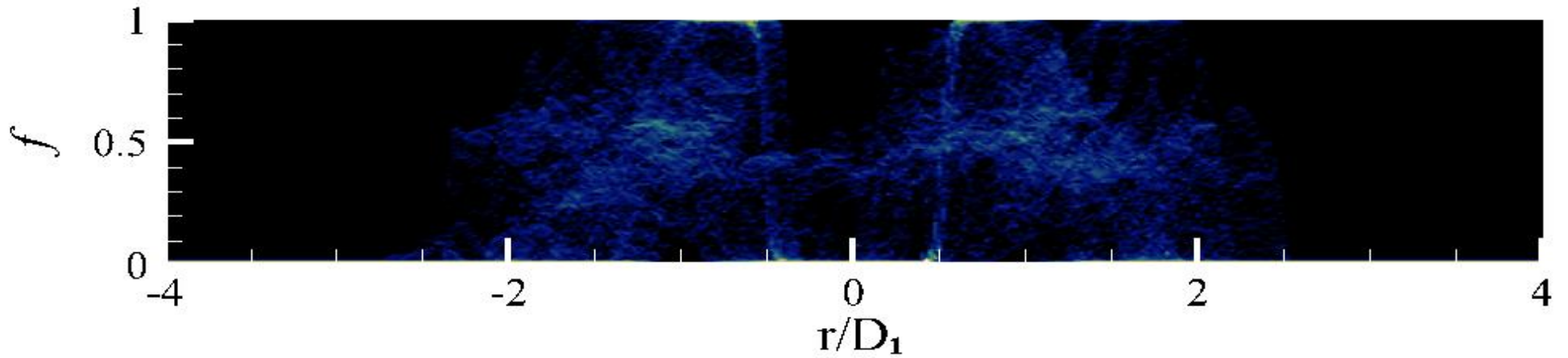
pdf:

0

33

67

100



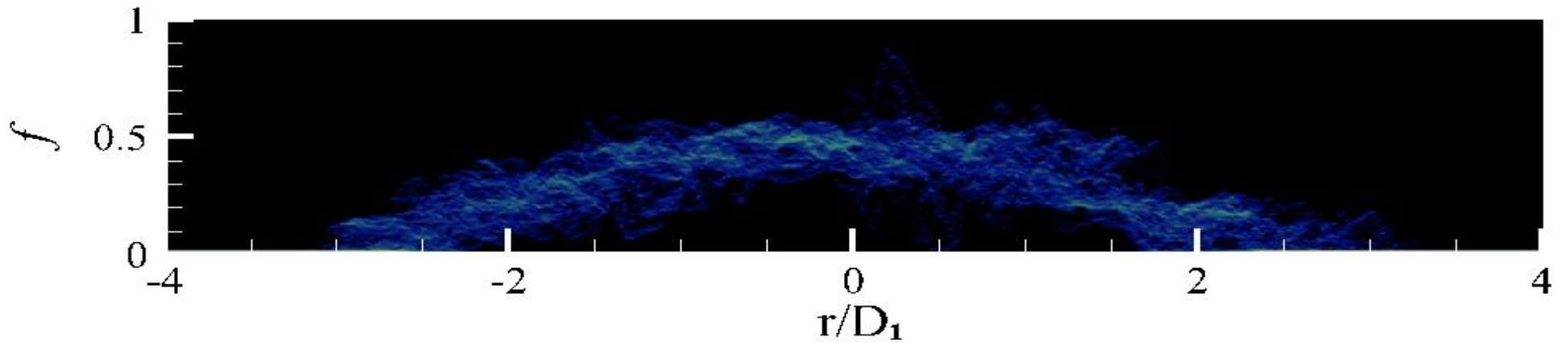
pdf:

0

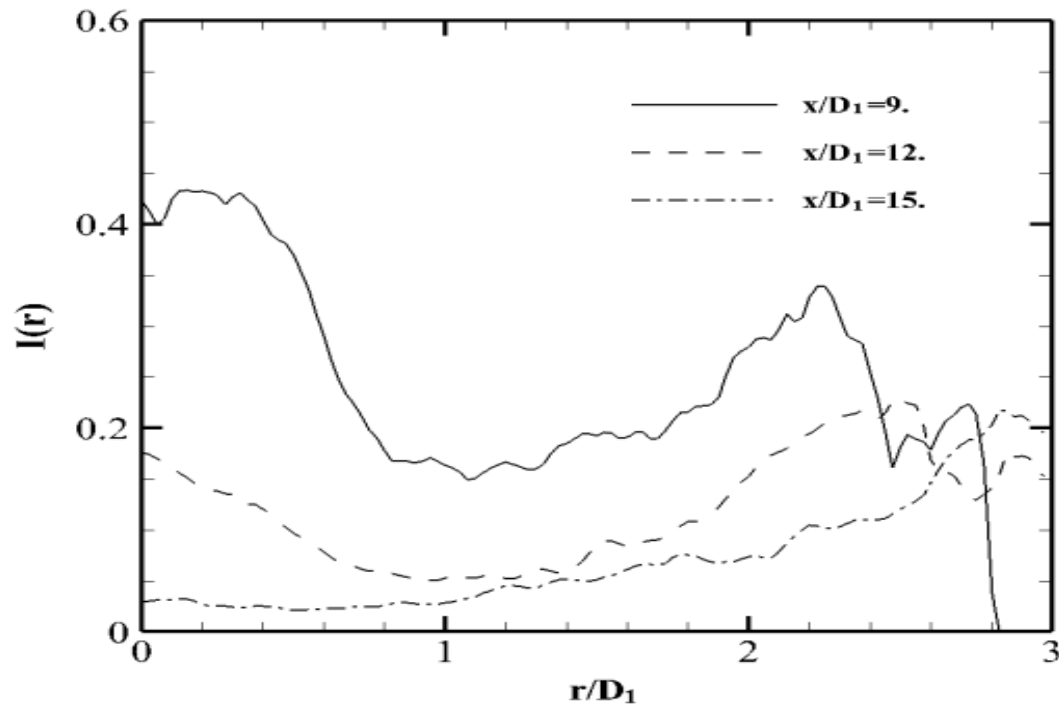
33

67

100



Variation of the probability density function of the mixture fraction (PDF) across the anisothermal jet at: a) $x/D_1 = 6$. b) $x/D_1 = 15$.



To have a better view of the mixing homogeneity after the end of the outer potential core. This quantity, introduced by Danckwerts is defined by:

$$\mathbf{I} = \frac{\langle \mathbf{f}'^2 \rangle}{\langle \mathbf{f} \rangle (1 - \langle \mathbf{f} \rangle)}$$

Certificate of Attendance

ORAL PRESENTATION

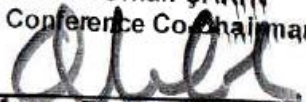
Name & Surname MOHAMED SI AMEUR

Paper Title NUMERICAL STUDY OF AIR-AIR MIXING IN TURBULENT COMPRESSIBLE COAXIAL JETS: EFFECT OF HOT JET

İÇAME 2019
5TH INTERNATIONAL CONFERENCE ON ADVANCES IN MECHANICAL ENGINEERING
DECEMBER 17-19, 2019
ISTANBUL



Assoc. Prof. Dr. Orhan ÇAKIR
ICAME 2019 Conference Co-Chairman


Assoc. Prof. Dr. Orhan ÇAKIR
YILDIZ TECHNICAL UNIVERSITY
Faculty of Mechanical Engineering
Vice Dean